ELSEVIER

European Journal of Pharmacology 376 (1999) 169–178

ejp

www.elsevier.nl/locate/ejphar

Effects of manidipine and nitrendipine enantiomers on the plateau phase of K^+-induced intracellular Ca^{2+} increase in GH_3 cells

Mauro Cataldi [a], Maurizio Taglialatela [a], Francesco Palagiano [b], Agnese Secondo [a], Paolo de Caprariis [c], Salvatore Amoroso [a], Gianfranco di Renzo [d], Lucio Annunziato [a,*]

[a] *Section of Pharmacology, Department of Neuroscience, School of Medicine, University of Naples Federico II, Via Pansini 5, 80131 Naples, Italy*
[b] *Department of Pharmaceutical and Toxicological Chemistry, University of Naples Federico II, Via Pansini 5, 80131 Naples, Italy*
[c] *Institute of Analytical Pharmaceutics, School of Pharmacy, University of Sassari, Sassari, Italy*
[d] *School of Pharmacy, University of Catanzaro, Catanzaro, Italy*

Received 2 November 1998; received in revised form 22 February 1999; accepted 26 February 1999

Abstract

The aim of the present study was to investigate whether the chirality and type of substitution at position 3 of the dihydropyridine ring influences the pattern of voltage-gated Ca^{2+} channel blockade. For this purpose, the effect of R- and S-enantiomers of manidipine and nitrendipine, separated by chiral High-Pressure-Liquid-Chromatography columns, were investigated by fura-2 microfluorimetry during the plateau phase of the intracellular Ca^{2+} ($[Ca^{2+}]_i$) increase induced by 55 mM K^+ and by patch-clamp recording of Ca^{2+} channel activity in GH_3 cells. R- and S-enantiomers of both nitrendipine and manidipine produced a $[Ca^{2+}]_i$ decay of the K^+-induced plateau phase that followed a biexponential pattern with a 'fast' and a 'slow' phase. The S-configuration of both nitrendipine and manidipine produced a larger $[Ca^{2+}]_i$ decrease during the 'fast phase', and a faster and smaller $[Ca^{2+}]_i$ decrease in the 'slow phase' than did the R-enantiomers. The S- and R-enantiomers of manidipine, which possess a longer and more lipophilic side chain at position 3 of the dihydropyridine ring, induced a slower $[Ca^{2+}]_i$ decrease than that observed with the respective nitrendipine enantiomers. Accordingly, patch-clamp experiments revealed that the S-enantiomers of both dihydropyridines displayed a faster onset of action and produced a greater blockade than the R-enantiomers. These results suggest that the enantiomeric configuration and a small side chain at position 3 of the dihydropyridine ring are factors in the chemical structure which influence the pattern of blockade of voltage-sensitive Ca^{2+} channels.

Keywords: Chirality; Dihydropyridine; Ca^{2+} concentration, intracellular; Nitrendipine; Manidipine; Ca^{2+} channel, voltage sensitive

1. Introduction

Although Ca^{2+} entry blockers of the dihydropyridine family share a common chemical structure and mechanism of action (Lee and Tsien, 1983; Hockermann et al., 1997), they display different pharmacological properties (Van Zwieten and Pfaffendorf, 1993). Some years ago, a great deal of effort was devoted to the study of the role of the chirality of the carbon at position 4 of the dihydropyridine ring (Goldmann and Stoltefuss, 1991) and to the study of the size and the lipophilicity of the substituents at positions 3 and 5 (Kojda et al., 1991), chemical properties which can affect the potency and tissue selectivity of dihydropyridines. For example, the S-(+) enantiomer of manidipine is about 30–80 times more potent than the R-(−) isomer in its antihypertensive action and in the radioligand binding assay (Kajino et al., 1989). The S-(−) enantiomer of nitrendipine is at least one order of magnitude more potent than the R-(+)-enantiomer in lowering diastolic blood pressure in human subjects (Mikus et al., 1995). In addition, lengthening of the ester chain at positions 3 and 5, as occurs in manidipine, can increase the receptor affinity and vascular selectivity of dihydropyridines (Triggle and Janis, 1987; Kojda et al., 1991).

In light of the chiral and chemical peculiarities of dihydropyridines, the aim of the present study was to investigate whether the chirality and type of substitution at position 3 of the dihydropyridine ring influence the pattern of voltage-sensitive Ca^{2+} channel (VSCC) blockade. For this purpose, the enantiomers of manidipine and nitrendipine, two chiral dihydropyridines which differ only in the

* Corresponding author. Tel.: +39-081-746-3318; fax: +39-081-746-3323; E-mail: farmacol@unina.it

0014-2999/99/$ - see front matter
PII: S0014-2999(99)00149-1

length and lipophilicity of the substituent at position 3 (Meguro et al., 1985; Goa and Sorkin, 1987; Eltze et al., 1990), were separated by means of chiral High-Pressure-Liquid-Chromatography columns (Tokuma et al., 1987; Delee et al., 1988; Okamoto et al., 1990; Stalcup et al., 1990). The effects of these enantiomers on the decrease in the intracellular Ca^{2+} concentration ($[Ca^{2+}]_i$) after high K^+-induced depolarization (Giovannelli and Pepeu, 1989) was continuously monitored by single-cell fura-2 microfluorimetry and by patch-clamp recordings in GH_3 cells, a pituitary clone provided with VSCC coupled to growth hormone and prolactin release (Ozawa and Kimura, 1982). The pattern of VSCC blockade by the two enantiomers of each dihydropyridine was compared in order to determine the role played by the chiral configuration. The effects of manidipine enantiomers were compared with those of their respective nitrendipine counterparts, in order to study the function exerted by the side chain at position 3.

2. Materials and methods

2.1. Separation of manidipine and nitrendipine enantiomers

Nitrendipine and manidipine enantiomers were isolated from their racemic mixtures using a direct phase High-Pressure-Liquid-Chromatography technique (Okamoto et al., 1990). Briefly, racemic nitrendipine and manidipine were dissolved in *n*-hexane/2-propanol (90:10) until a saturated solution was obtained. This solution was then filtered using Millipore Millex-HV filters (Millipore, Molsheim, France) and injected through a Waters Associates WISP 700 Autoinjector into a Waters Associates High-Pressure-Liquid-Chromatography apparatus with a 600E pump (Waters Associates, Milford, MA). Manidipine and nitrendipine enantiomers were injected into a Daicel Chiralpak AD column (4.6 × 250 mm) with a Daicel Chiralpak AD pre-column (4.6 × 50 mm) (Daicel Chemical Industries, Tokyo, Japan) under isocratic conditions, at a flow rate of 0.5 ml/min. In order to separate manidipine enantiomers, the column was eluted with a 83:17 *n*-hexane/2-propanol mixture, while nitrendipine enantiomers were separated using a 90:10 *n*-hexane/2-propanol mixture.

Eluting peaks were identified by continuously monitoring the eluate absorbance at 240 nm with a Waters Associates UV-vis Detector 486 (Waters Associates). The temperature of the High-Pressure-Liquid-Chromatography apparatus was kept at 25°C using a Waters Associates temperature control module. The pump, the injector and the detector were controlled by a NEC Powermate SX/16 computer (NEC, Tokyo, Japan).

In order to obtain a sufficient amount of each enantiomer, multiple and time-scheduled injections of the racemic mixture were performed during the same High-

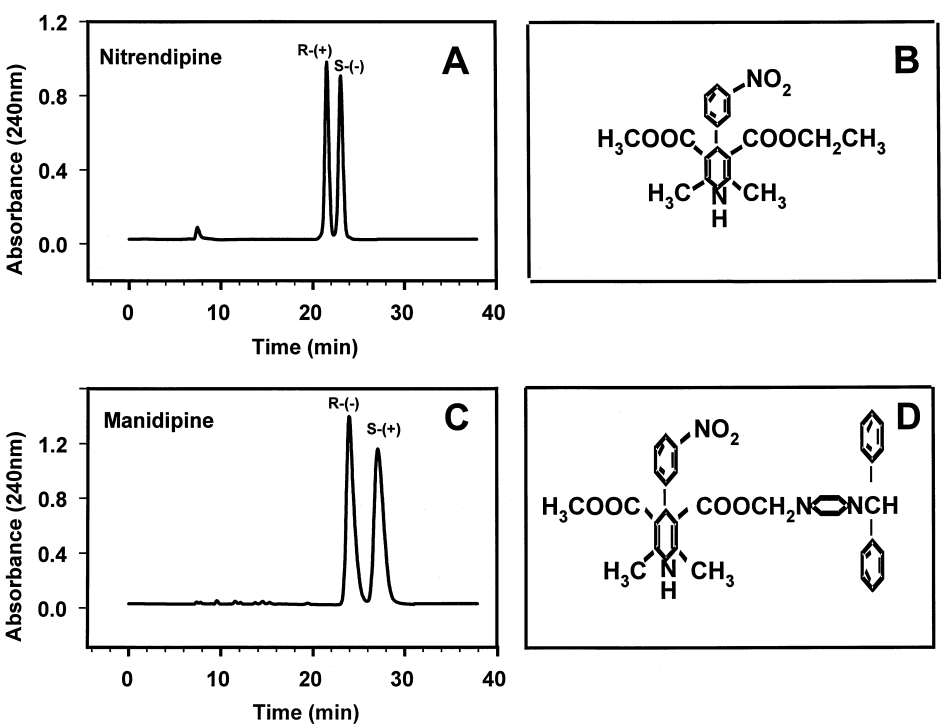

Fig. 1. High-Pressure-Liquid-Chromatography separation of nitrendipine and manidipine enantiomers. Nitrendipine and manidipine racemates were injected into a High-Pressure-Liquid-Chromatography apparatus provided with a chiral column and separated as described in Section 2. Panel A and C show the absorbance profile of nitrendipine and manidipine enantiomers, respectively, obtained by the continuous spectrophotometric monitoring of the column eluate. Panel B and D show the chemical structures of nitrendipine and manidipine, respectively.

Pressure-Liquid-Chromatography session. Multiple injections were performed every 6 min for manidipine and every 5 min for nitrendipine. The eluted enantiomers were collected in dark glass tubes and dried under nitrogen at room temperature to eliminate the eluant mixture.

The polarimetric measurements were performed using a Perkin Elmer 243 B Polarimeter (Perkin Elmer, Foster City, CA, USA).

2.2. Cell culture

GH_3 cells were obtained from Flow Laboratories (Irvine, Scotland) and grown on plastic dishes in Ham's F10 medium (Gibco-BRL, San Giuliano Milanese, Italy) composed of 15% horse serum (Flow, Irvine, Scotland), 2.5% fetal calf serum (Hyclone, Logan, UT, USA), 100 I.U. of penicillin/ml, and 100 μg of streptomycin/ml. The cells were cultured in a humidified 5% CO_2 atmosphere and the culture medium was changed every 2 days. For microfluorimetric studies, the cells were seeded on glass coverslips (Fisher, Springfield, NJ, USA) coated with poly-L-lysine (30 μg/ml) (Sigma, St. Louis, MO, USA) and used at least 12 h after seeding.

2.3. Intracellular calcium measurements

$[Ca^{2+}]_i$ was measured using a microfluorimetric technique, as previously reported (Cataldi et al., 1996). Briefly, the cells grown on glass coverslips were loaded with 5 μM 1-[2-(5-carboxyoxazol-2-yl)-6-aminobenzofuran-5-oxy]-2-2^1-amino-5^1-methylphenoxy)-ethane-*N*,*N*,*N*^{1},*N*^{1}-tetraacetic acid pentaacetoxymethyl ester (fura-2AM) in Krebs–Ringer saline solution (5.5 mM KCl, 160 mM NaCl, 1.2 mM $MgCl_2$, 1.5 mM $CaCl_2$, 10 mM glucose, and 10 mM Hepes-NaOH, pH 7.4) for 1 h at room temperature. At the end of fura-2AM loading, the coverslip was introduced into a microscope chamber (Medical System, Greenvale, NY) on an inverted Nikon Diaphot fluorescence microscope. The cells were kept in Krebs–Ringer saline solution throughout the experiment. All the drugs tested were introduced into the microscope chamber by fast injection. When the depolarizing extracellular K^+ solution (55 mM) was used, the osmolarity of the solution was kept constant by accordingly reducing the extracellular Na^+ concentration. A 100-W Xenon Lamp (Osram, Germany) with a computer-operated filter wheel bearing two different interference filters (340 and 380 nm) illuminated the microscopic field with UV light, alternating the wavelength at an interval of 500 ms. The interval between each pair of illuminations was 2 s, and the interval between filter movements was 1 s. Consequently, $[Ca^{2+}]_i$ was measured every 3 s. Emitted light was passed through a 400-nm dichroic mirror, filtered at 510 nm, and collected by a CCD camera (Photonic Science, Robertsbridge, East Sussex, UK) connected to a light amplifier (Applied Imaging, Dukesway Gateshead, UK). Images were digitized and analyzed with a Magiscan image processor (Applied Imaging). Using a calibration curve, the Tardis software (Applied Imaging) calculated the $[Ca^{2+}]_i$ corresponding to each pair of images from the ratio between the intensity of the light emitted when the cells were illuminated at both 340 and 380 nm.

2.4. Patch-clamp recordings

Currents from GH_3 cells were recorded at room temperature using a commercially available amplifier (Axopatch 200A, Axon Instruments, Foster City, CA). The whole-cell configuration of the patch-clamp technique (Hamill et al., 1981) was used with glass micropipettes of 3–7 MΩ resistance. No compensation was made for pipette resistance and cell capacitance. The cells were perfused with an extracellular solution containing (in mM): 10 $BaCl_2$, 0.125 NaCl, 1 $MgCl_2$, 10 HEPES, 300 nM Tetrodotoxin, pH 7.3. The pipettes were filled with (in mM): 110 CsCl, 10 tetraethylammonium-Cl, 2 $MgCl_2$, 10 EGTA, 8 glucose, 2 Mg-ATP, 0.25 cAMP and 10 HEPES, pH 7.3. Current flowing through voltage-dependent Ca^{2+} channels was activated by continuous ramp pulses from −100 to

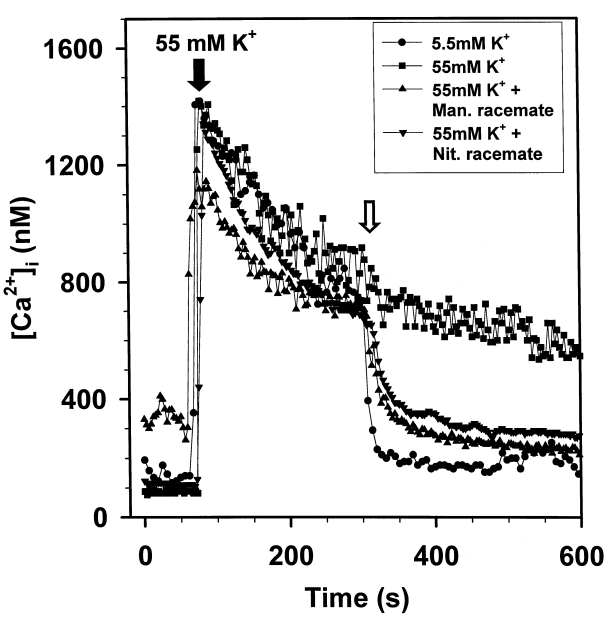

Fig. 2. Effect of 55 mM K, 5.5 mM K^+, 55 mM K^+ + manidipine and 55 mM K^+ + nitrendipine racemates on $[Ca^{2+}]_i$ decay during the plateau phase of the 55 mM K^+-induced $[Ca^{2+}]_i$ response. K^+ (55 mM) was added to the incubation medium after 70 s of baseline $[Ca^{2+}]_i$ monitoring, as indicated by the black arrow. Then, 220 s later, as indicated by the white arrow, the incubation medium was replaced with new medium containing either 5.5 mM K^+ (●) or 55 mM K^+ alone (■), or 55 mM K^+ with 100 nM manidipine racemate (▲) or 55 mM K^+ with 100 nM nitrendipine racemate (▼). The traces shown are the means of at least 15 cells recorded during a single experimental session representative of at least three different experiments.

+60 mV (32 ms/pulse, 100 μs/sampling point) elicited at 0.08 Hz frequency (one pulse every 12 s). The Ba^{2+} current through Ca^{2+} channels was obtained by subtracting the current elicited with identical protocols in the presence of 50 μM $CdSO_4$.

2.5. Drugs and chemicals

Chemicals were of analytical grade and were purchased from Sigma (Sigma Italia, Milan, Italy). Fura 2-AM was acquired from Calbiochem (La Jolla, CA, USA). Nitrendipine was a generous gift of Bayer (Bayer Leverkusen, Germany), while manidipine was obtained from commercial sources.

2.6. Statistical analysis of the data

All the data are expressed as means ± S.E.M. The statistical analysis was performed using the Student's *t*-test for paired or unpaired data, where required. The threshold for statistical significance was set at $P < 0.05$. The $[Ca^{2+}]_i$ decay occurring when GH_3 cells depolarized with high K^+ concentrations were exposed to physiological K^+ concentrations or to increasing concentrations of dihydropyridines was fitted to monoexponential ($y = a + b \cdot e^{(-t/\tau)}$) or to the biexponential ($y = a + b \cdot e^{(-t/\tau 1)} + c \cdot e^{(-t/\tau 2)}$) equations using Nfit software (University of Texas at Galveston, TX, USA). In these equations, τ represents the time constant for decay, while *b* and *c* are a measure of the

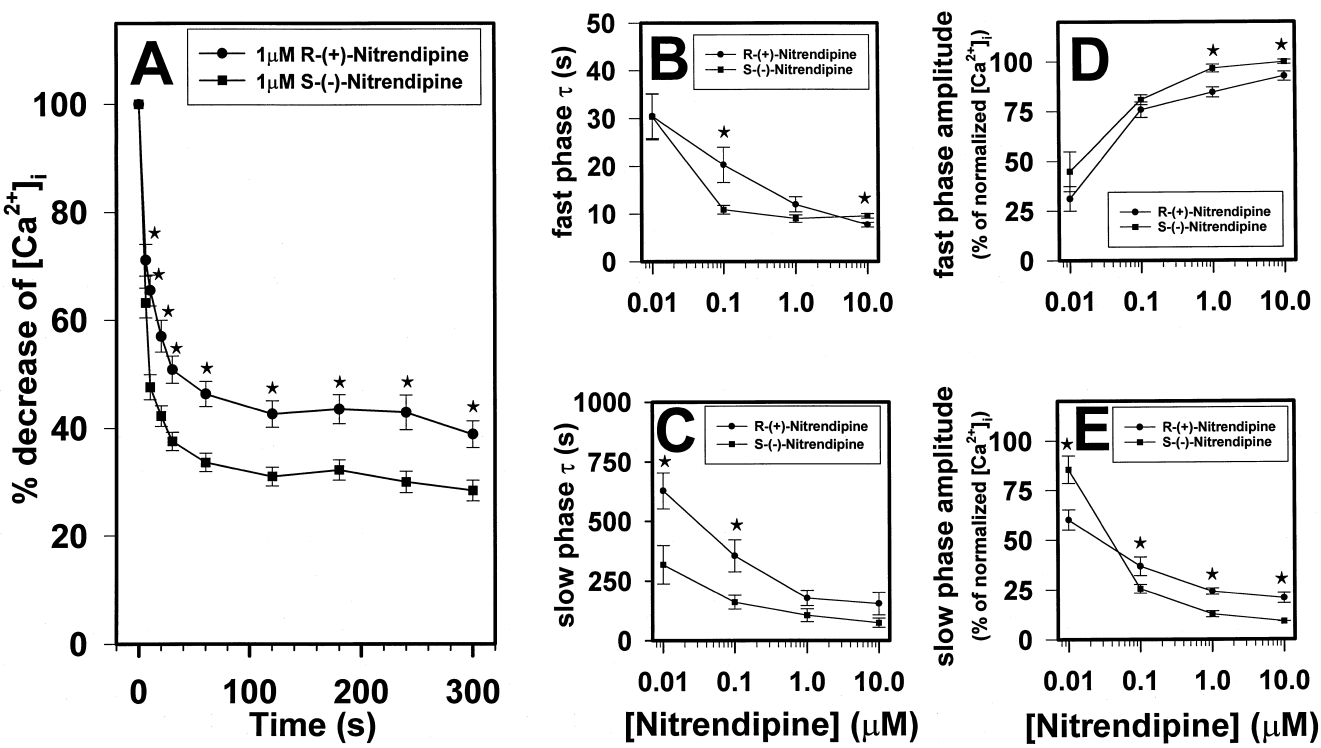

Fig. 3. $[Ca^{2+}]_i$ decay induced by R-(+)- and S-(−)-nitrendipine enantiomers added during the plateau phase of the 55 mM K^+-induced $[Ca^{2+}]_i$ response. Panel A shows the decrease of $[Ca^{2+}]_i$ induced by 55 mM K^+ plus 1 μM R-(+)-(●) or 1 μM S-(−)-(■) nitrendipine added during the plateau phase. According to the protocol described in the legend of Fig. 2, GH_3 cells were depolarized with 55 mM K^+. Then, 55 mM K^+ plus either 1 μM R-(+)-(●) or 1 μM S-(−)-nitrendipine (■) was added 220 s after the beginning of the K^+ pulse. In this figure only, the dihydropyridine-induced $[Ca^{2+}]_i$ decay of the 55 mM K^+-induced plateau phase is represented, and the peak phase of K^+-induced $[Ca^{2+}]_i$ elevation previously shown in Fig. 2 is omitted. Values are expressed as percentages of $[Ca^{2+}]_i$ values observed just before dihydropyridine addition. The asterisk indicates $P < 0.05$ vs. the respective time point for the other enantiomer. Panel B shows the values for the kinetic constant τ of the 'fast phase' of the biexponential decay induced by increasing concentrations of R-(+)-(●) and S-(−)-(■) nitrendipine. Panel C shows the values for the kinetic constant τ of the 'slow phase' of the biexponential decay induced by increasing concentrations of R-(+)-(●) and S-(−)-(■) nitrendipine. Panel D shows the magnitude of $[Ca^{2+}]_i$ decay induced by increasing concentrations of R-(+)-(●) and S-(−)-(■) nitrendipine during the 'fast phase' of the biexponential $[Ca^{2+}]_i$ decay. In order to normalize the magnitude values, the data are expressed as percentages of the $[Ca^{2+}]_i$ values recorded just before dihydropyridine addition according to the following formula: magnitude $= (b/([Ca^{2+}]_{i\ -\ init.} - a)) \cdot 100$ where $[Ca^{2+}]_{i-init.}$ is the $[Ca^{2+}]_i$ recorded just before dihydropyridine addition, *b* is the fast-phase magnitude constant and *a* is the $[Ca^{2+}]_i$ at time = $+\infty$ in the biexponential equation $[Ca^{2+}]_i = a + b \cdot e^{-t/t1} + c \cdot e^{-t/t2}$. Panel E shows the magnitude of $[Ca^{2+}]_i$ decay induced by increasing concentrations of R-(+)-(●) and S-(−)-(■) nitrendipine during the 'slow phase' of the biexponential $[Ca^{2+}]_i$ decay. In order to normalize the magnitude values, the data are expressed as percentages of the $[Ca^{2+}]_i$ values recorded just before dihydropyridine addition according to the following formula: magnitude $= (c/([Ca^{2+}]_{i\ -\ init.} - a)) \cdot 100$ where $[Ca^{2+}]_{i-init.}$ is the $[Ca^{2+}]_i$ recorded just before dihydropyridine addition, *c* is the fast-phase magnitude constant and *a* is the $[Ca^{2+}]_i$ at time = $+\infty$ in the biexponential equation $[Ca^{2+}]_i = a + b \cdot e^{-t/t1} + c \cdot e^{-t/t2}$. For each enantiomer concentration, the *t* and magnitude values reported are the means ± S.E.M. for 30–50 single cell values obtained in at least three different experimental sessions. The asterisk indicates $P < 0.05$ vs. the same concentration of the other enantiomer.

magnitude of this decay from the values recorded at the beginning. The kinetic data reported in the present study are the means ± S.E.M. of single-cell fitting determinations obtained by the analysis of all the cells recorded in each of the different experimental sessions.

3. Results

3.1. Separation parameters of nitrendipine and manidipine R- and S-enantiomers

As shown in Fig. 1, the R-enantiomers of nitrendipine and manidipine eluted before the S-enantiomers. The enantiomers of each dihydropyridine were completely separated. In fact, the α and Rs values for nitrendipine were 1.16 and 1.12, respectively, and 1.17 and 1.46 in the case of manidipine. The α values were obtained by the equation $\alpha = k'_2 - k'_1$ where $k' = (t - t_0)/t_0$. t_0 represents the retention time of an unretained substance. The Rs value was calculated by the equation $Rs = 2(t_2 - t_1)/(W_1 - W_2)$, where t_1 and t_2 are the retention times of the first and the second enantiomers to be eluted, and W represents the width of the peak measured at its base. The purity of each enantiomer, assessed by reinjection into the High-Pressure-Liquid-Chromatography column, was more than 95% for each enantiomer.

3.2. Effect of nitrendipine and manidipine racemic mixtures on $[Ca^{2+}]_i$ decay during the plateau phase of the 55 mM K^+-induced $[Ca^{2+}]_i$ increase in GH_3 cells

When GH_3 cells were exposed to a depolarizing concentration of K^+ ions (55 mM), a sudden increase of $[Ca^{2+}]_i$ occurred. This peak was followed by a long-lasting plateau phase (Fig. 2). Replacement of 55 mM K^+ containing Krebs–Ringer solution by 55 mM K^+ solution containing the racemate of either nitrendipine or manidipine (100 nM) led to a decay of $[Ca^{2+}]_i$. This dihydropyridine-induced decay consisted of a 'fast phase' of approximately 20–30″ followed by a much longer 'slow phase' lasting several minutes. Similarly, the replacement of 55 mM K^+ by a solution containing physiological concentrations of K^+ ions (5.5 mM) caused a rapid decline of $[Ca^{2+}]_i$ to baseline values (Fig. 2). When 55 mM K^+ was replaced by a solution containing 55 mM K^+ ions plus the inorganic VSCC blocker Cd^{2+} (200 μM), a rapid decline of $[Ca^{2+}]_i$ to baseline values was also observed

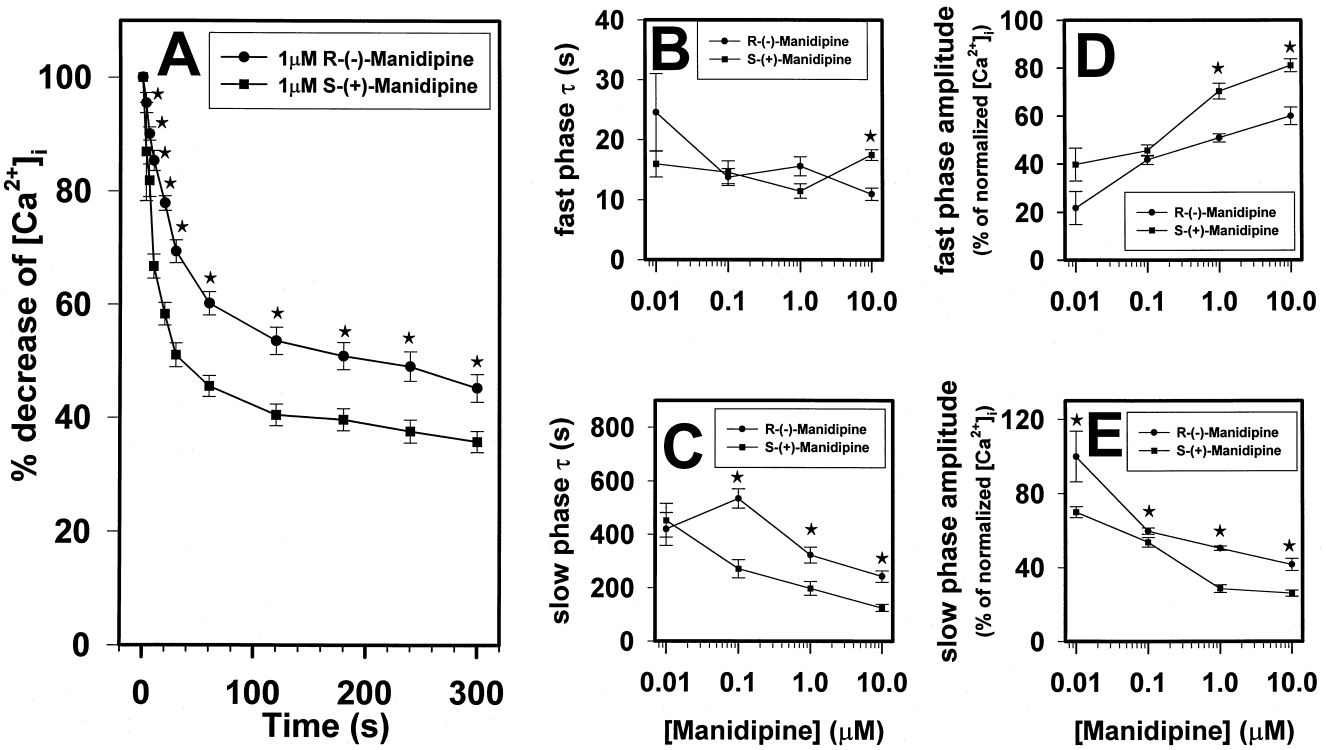

Fig. 4. $[Ca^{2+}]_i$ decay induced by R-(−)- and S-(+)-manidipine added during the plateau phase of the 55 mM K^+-induced $[Ca^{2+}]_i$ response. Panel A shows the decrease of $[Ca^{2+}]_i$ induced by 55 mM K^+ plus 1 μM R-(−)-(●) or 1 μM S-(+)-(■) manidipine when added during the plateau phase of the 55 mM K^+-induced $[Ca^{2+}]_i$ response. Panel B shows the values for the kinetic constant τ of the 'fast phase' of the biexponential decay induced by increasing concentrations of R-(−)-(●) and S-(+)-(■) manidipine. Panel C shows the values for the kinetic constant τ of the 'slow phase' of the biexponential decay induced by increasing concentrations of R-(−)-(●) and S-(+)-(■) manidipine. Panel D shows the magnitude of the $[Ca^{2+}]_i$ decay induced by increasing concentrations of R-(−)-(●) and S-(+)-(■) manidipine during the 'fast phase' of the biexponential $[Ca^{2+}]_i$ decay. Panel E shows the magnitude of $[Ca^{2+}]_i$ decay induced by increasing concentrations of R-(−)-(●) and S-(+)-(■) manidipine during the 'slow phase' of the biexponential $[Ca^{2+}]_i$ decay. For experimental details, see the legend of Fig. 3.

(data not shown). The decrease of the 55 mM K^+-induced $[Ca^{2+}]_i$ elevation during the plateau phase brought about by 5.5 mM K^+ plus dihydropyridine racemates shows that a consistent percentage of VSCC are still open during the K^+-induced plateau phase and can be therefore blocked by the addition of dihydropyridines. The kinetics of the $[Ca^{2+}]_i$ decay induced by dihydropyridines can be fitted to a biexponential curve characterized by two parameters for each phase, the magnitude and the time constant τ. The analysis of these two kinetic phases of dihydropyridine-induced VSCC blockade makes it possible to identify differences in the pattern of VSCC blockade among different dihydropyridine enantiomers.

3.3. Effect of R-(+) and S-(−)-nitrendipine on $[Ca^{2+}]_i$ decay during the plateau phase of the 55 mM K^+-induced $[Ca^{2+}]_i$ increase in GH_3 cells

According to the above-mentioned model of dihydropyridine activity evaluation, R or S nitrendipine enantiomers were added 220 s after the beginning of the 55 mM K^+ pulse (time 0 of Fig. 3A). Both nitrendipine enantiomers induced a decrease of $[Ca^{2+}]_i$ that could be fitted to biexponential equations with a 'fast phase' followed by a 'slow phase' (Fig. 3A). 'Fast phase' τ values for the R-(+)- and S-(−)-nitrendipine enantiomers were significantly different at concentrations of 0.1 and 10 μM (Fig. 3B). 'Slow phase' τ values for R-(+)-nitrendipine were significantly higher than those for S-(−)-nitrendipine at concentrations of 0.01 and 0.1 μM (Fig. 3C). Furthermore, the magnitude of $[Ca^{2+}]_i$ decay induced by S-(−)-nitrendipine during the 'fast phase' was significantly greater than that induced by R-(+)-nitrendipine at the concentrations of 1–10 μM (Fig. 3D). By contrast, the magnitude of $[Ca^{2+}]_i$ decay induced by S-nitrendipine during the 'slow phase' was significantly lower at concentrations of 0.1, 1 and 10 μM (Fig. 3E).

3.4. Effect of R-(−) and S-(+)-manidipine on $[Ca^{2+}]_i$ decay during the plateau phase of the 55 mM K^+-induced $[Ca^{2+}]_i$ increase in GH_3 cells

The addition of S-(+) and R-(−)-manidipine enantiomers 220 s after the beginning of the 55 mM K^+ pulse induced a biexponential decay of $[Ca^{2+}]_i$ (Fig. 4A). 'Fast phase' τ values for the S-(+)- and R-(−)-manidipine enantiomers were not significantly different at the concentrations used (0.01, 0.1 and 1 μM). At 10 μM, the

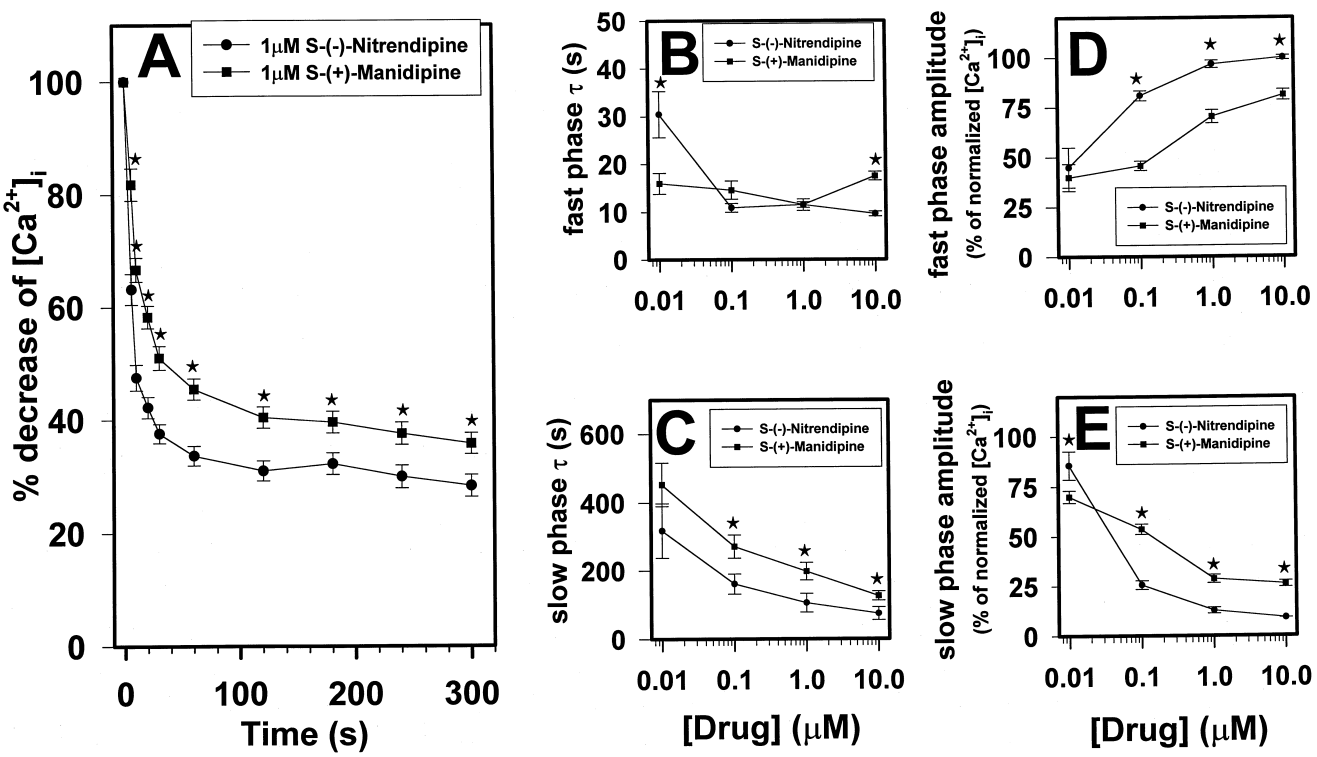

Fig. 5. $[Ca^{2+}]_i$ decay induced by S-(−)-nitrendipine and S-(+)-manidipine added during the plateau phase of the 55 mM K^+-induced $[Ca^{2+}]_i$ response. Panel A shows the decrease of $[Ca^{2+}]_i$ induced by 55 mM K^+ plus 1 μM S-(−)-nitrendipine (●) or 1 μM S-(+)-manidipine (■) when added during the plateau phase of the 55 mM K^+-induced $[Ca^{2+}]_i$ response. Panel B shows the values for the kinetic constant τ of the 'fast phase' of the biexponential decay induced by increasing concentrations of S-(−)-nitrendipine (●) and S-(+)-manidipine (■). Panel C shows the values for the kinetic constant τ of the 'slow phase' of the biexponential decay induced by increasing concentrations of S-(−)-nitrendipine (●) and S-(+)-manidipine (■). Panel D shows the magnitude of $[Ca^{2+}]_i$ decay induced by increasing concentrations of S-(−)-nitrendipine (●) and S-(+)-manidipine (■) during the 'fast phase' of the biexponential $[Ca^{2+}]_i$ decay. Panel E shows the magnitude of $[Ca^{2+}]_i$ decay induced by increasing concentrations of S-(−)-nitrendipine (●) and S-(+)-manidipine (■) during the 'slow phase' of the biexponential $[Ca^{2+}]_i$ decay. For experimental details, see the legend of Fig. 3.

S-(+)-enantiomer 'fast phase' τ value was higher (Fig. 4B). The τ values for R-(−)-manidipine during the 'slow phase' were significantly higher than those for the respective S-(+)-enantiomer at 0.1, 1, and 10 μM (Fig. 4C). In addition, the magnitude of the $[Ca^{2+}]_i$ decrease induced by S-(+)-manidipine during the 'fast phase' was greater than that induced by R-(−)-manidipine at concentrations of 1 and 10 μM (Fig. 4D). Yet, at concentrations of 0.01, 0.1, 1 and 10 μM, the magnitude of the decay of $[Ca^{2+}]_i$ induced by R-(−)-manidipine during the 'slow phase' was greater than that induced by the S-(+)-enantiomer (Fig. 4E).

3.5. Comparison of the amplitude and τ values of the S- and R-enantiomers of manidipine and their nitrendipine counterparts

Time-course analysis of the effects of S-(−)-nitrendipine and S-(+)-manidipine on $[Ca^{2+}]_i$ decay after 55 mM K^+ showed that S-(−)-nitrendipine was significantly faster acting than S-(+)-manidipine at all the times considered (Fig. 5A). The τ values for the 'fast phase' of S-(+)-manidipine were lower than those of S-(−)-nitrendipine at concentrations of 0.01 and 10 μM (Fig. 5B) and the 'slow phase' τ value of S-(+)-manidipine was higher than that of S-(−)-nitrendipine at concentrations of 0.1, 1 and 10 μM (Fig. 5C). The magnitude of the 'fast phase' of $[Ca^{2+}]_i$ decay after S-(−)-nitrendipine was greater than that of S-(+)-manidipine at concentrations of 0.1, 1, and 10 μM (Fig. 5D). By contrast, the magnitude of the 'slow phase' $[Ca^{2+}]_i$ decline was greater for S-(+)-manidipine at concentrations of 0.1, 1, and 10 μM (Fig. 5E).

Time-course analysis of R-(+)-nitrendipine and R-(−)-manidipine-induced $[Ca^{2+}]_i$ decay after 55 mM K^+ showed that the effect of R-(+)-nitrendipine occurred significantly faster than that of R-(−)-manidipine (Fig. 6A). The τ values for the 'fast phase' were not statistically different for R-(+)-nitrendipine and R-(−)-manidipine except at the highest concentration (10 μM) (Fig. 6B), while the time constant τ values for the 'slow phase' were higher for R-(−)-manidipine than for R-(+)-nitrendipine at concentrations of 0.1 and 1 μM (Fig. 6C).

The magnitude of the $[Ca^{2+}]_i$ decline induced by R-(+)-nitrendipine during the 'fast phase', was greater than that induced by R-(−)-manidipine, whereas the opposite was observed during the 'slow phase' (Fig. 6D and E).

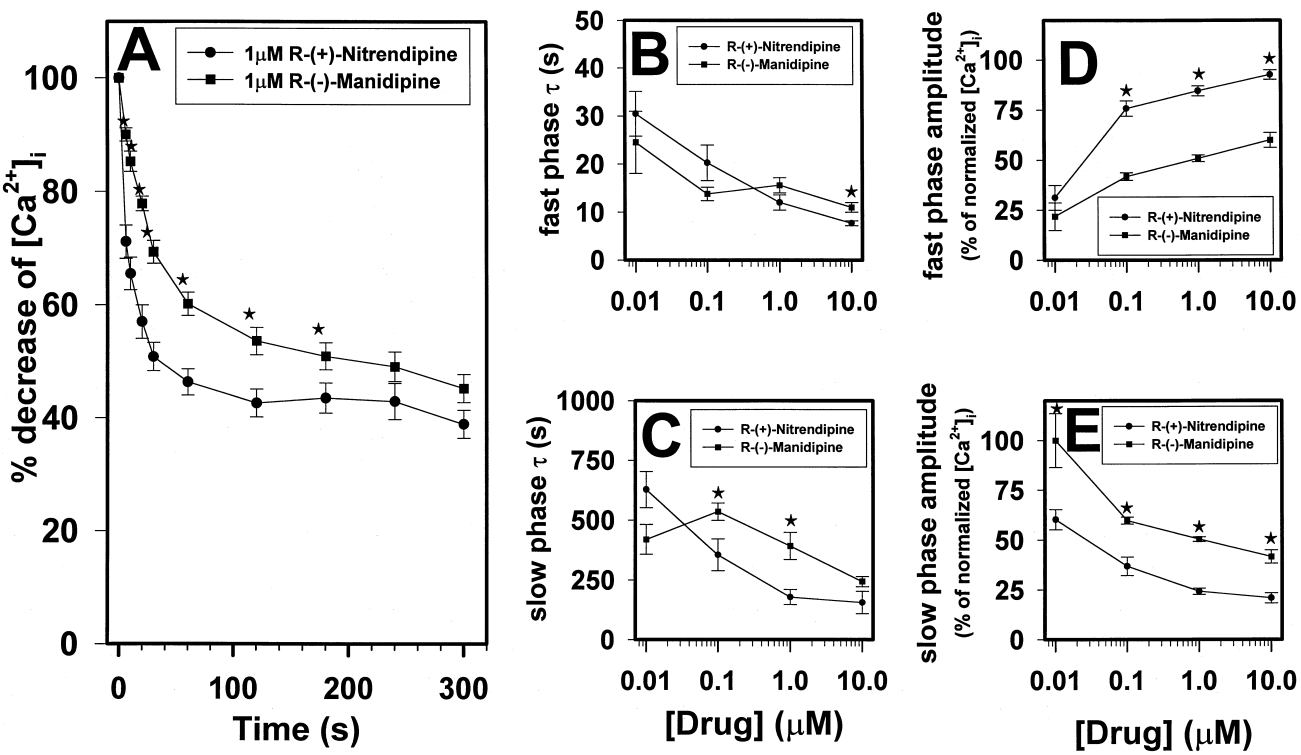

Fig. 6. $[Ca^{2+}]_i$ decay induced by R-(+)-nitrendipine and R-(−)-manidipine added during the plateau phase of the 55 mM K^+-induced $[Ca^{2+}]_i$ response. Panel A shows the decrease of $[Ca^{2+}]_i$ induced by 55 mM K^+ plus 1 μM R-(+)-nitrendipine (●) or 1 μM R-(−)-manidipine (■) when added during the plateau phase of 55 mM K^+-induced $[Ca^{2+}]_i$ response. Panel B shows the values for the kinetic constant τ of the 'fast phase' of the biexponential decay induced by increasing concentrations of R-(+)-nitrendipine (●) and R-(−)-manidipine (■). Panel C shows the values for the kinetic constant τ of the 'slow phase' of the biexponential decay induced by increasing concentrations of R-(+)-nitrendipine (●) and R-(−)-manidipine (■). Panel D shows the magnitude of $[Ca^{2+}]_i$ decay induced by increasing concentrations of R-(+)-nitrendipine (●) and R-(−)-manidipine (■) during the 'fast phase' of the biexponential $[Ca^{2+}]_i$ decay. Panel E shows the magnitude of $[Ca^{2+}]_i$ decay induced by increasing concentrations of R-(+)-nitrendipine (●) and R-(−)-manidipine (■) during the 'slow phase' of the biexponential $[Ca^{2+}]_i$ decay. For experimental details, see the legend of Fig. 3.

3.6. Effect of the R- and S-enantiomers of nitrendipine and manidipine on Ca^{2+} channel function detected by patch-clamp recordings in GH_3 cells

In patch-clamped GH_3 cells, voltage ramps from −100 to +60 mV revealed high voltage-activated Ba^{2+} currents mainly represented by the L-subtype VSCC (Cataldi et al., 1996) (Figs. 7A and 8A, B). Under control conditions, Ca^{2+} channel activity showed a slow progressive decline ('rundown') of about 15% during 274 s of recording (Figs. 7C and 8C). These inward currents were completely eliminated by 50 μM Cd^{+} perfusion (Figs. 7C and 8C). The application of the S-nitrendipine enantiomer (10 μM) caused a biphasic decline of Ca^{2+} channel activity with a 'fast' and a 'slow' phase, qualitatively similar to that found in the microfluorimetric studies (Fig. 7C). A 60% reduction of the peak inward Ba^{2+} current, occurring at ≈0 mV, was seen after 2 min of perfusion of the S-nitrendipine enantiomer. By contrast, the R-nitrendipine enantiomer displayed slower blocking kinetics, and after 2 min of superfusion the peak inward Ba^{2+} current was inhibited by about 30%. The kinetics of VSCC blockade by the S- and R-enantiomers of manidipine were similar to those of the corresponding nitrendipine enantiomers (Fig. 8A, B, and C). Furthermore, upon drug removal, the magnitude of VSCC blockade remaining after the previous exposure to the S-enantiomer of manidipine was greater than that occurring with the S-enantiomer of nitrendipine (Figs. 7C and 8C).

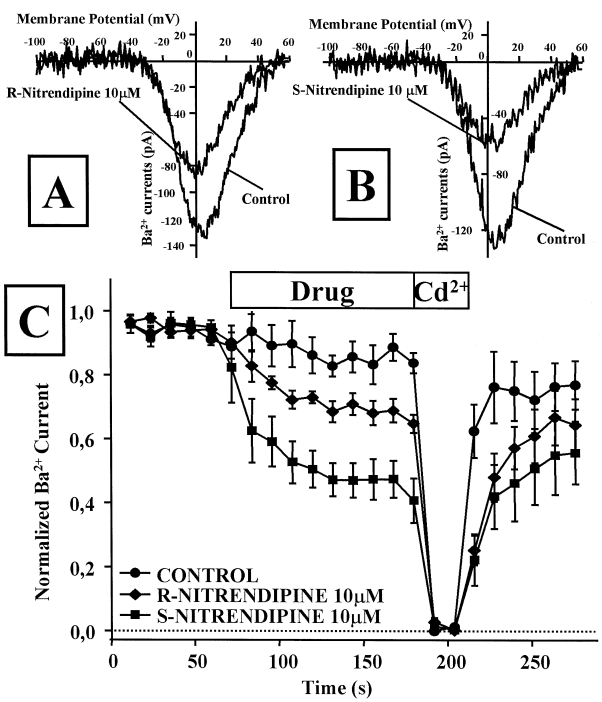

Fig. 7. Effect of R-(+)- and S-(−)-nitrendipine enantiomers on Ba^{2+} currents flowing through VSCC in GH_3 cells. Ba^{2+} currents flowing through voltage-dependent Ca^{2+} channels were activated by ramp pulses from −100 to +60 mV (32 ms/pulse, 100 μs/sampling point) elicited at 0.08 Hz frequency (one pulse every 12 s). The traces shown in panels A and B represent control and drug effect after 2 min of perfusion with 10 μM R- and S-nitrendipine, respectively. Each trace was obtained by subtracting the current elicited with identical protocols in the presence of 50 μM $CdSO_4$. In panel C, the time course of the peak Ba^{2+} currents flowing through voltage-dependent Ca^{2+} channels at ≈0 mV in the three experimental groups (control ●, 10 μM R-nitrendipine ♦, and 10 μM S-nitrendipine ■) is reported. The bar on the top of the panel indicates the duration of the drug exposure or of the Cd^{2+} perfusion in all three experimental groups.

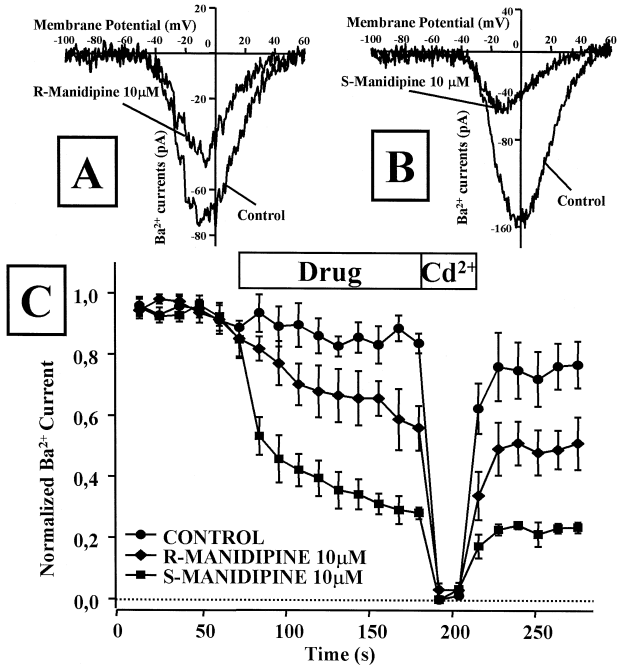

Fig. 8. Effect of R-(−)- and S-(+)-manidipine enantiomers on Ba^{2+} currents flowing through VSCC in GH_3 cells. Ba^{2+} currents flowing through voltage-dependent Ca^{2+} channels were activated by ramp pulses from −100 mV to +60 mV (32 ms/pulse, 100 μs/sampling point) elicited at 0.08 Hz frequency (one pulse every 12 s). The traces shown in panels A and B represent control and drug effect after 2 min perfusion with 10 μM R- and S-manidipine, respectively. Each trace was obtained by subtracting the current elicited with identical protocols in the presence of 50 μM $CdSO_4$. In panel C, the time course of the peak Ba^{2+} currents flowing through voltage-dependent Ca^{2+} channels at ≈0 mV in the three experimental groups (control ●, 10 μM R-manidipine ♦, and 10 μM S-manidipine ■) is reported. The bar on the top of the panel indicates the duration of the drug exposure or of the Cd^{2+} perfusion in all three experimental groups.

4. Discussion

The results of the present study showed that some L-type VSCCs are still in an open state and can be blocked by dihydropyridines during the plateau phase of $[Ca^{2+}]_i$ decay which follows the K^+-induced $[Ca^{2+}]_i$ peak phase. This was further demonstrated by the finding that both the replacement of extracellular depolarizing (55 mM) K^+ concentrations by physiological amounts of this cation (5 mM) and the application of the inorganic VSCC blocker

Cd^{2+} (data not shown) during the 'plateau phase' caused, as with dihydropyridines application, an abrupt decrease of $[Ca^{2+}]_i$ to baseline values. In line with this evidence, it has been demonstrated by Keller and Nussinovitch (1996), with the use of whole-cell patch-clamp recordings, that the VSCCs of anterior pituitary cells undergo 'ultraslow inactivation' during long-lasting depolarizations. Analogously, it has been demonstrated that at the resting membrane potential of −43 mV, a value at which most voltage-sensitive Ca^{2+} channels should be inactivated, a steady-state dihydropiridine-sensitive Ca^{2+} channel current can be still detected (Scherubl and Hescheler, 1991). Thus, the present experimental set-up, in which the effects of dihydropyridines are determined when the $[Ca^{2+}]_i$ decline is slow, may allow the detection of differences among dihydropyridine and/or their enantiomers in the pattern of the blockade of VSCC undergoing ultraslow inactivation. This would not be possible if dihydropyridines were added before the depolarizing stimulus or during the K^+-induced $[Ca^{2+}]_i$ peak, because the kinetics of $[Ca^{2+}]_i$ changes would be too fast. With the present set-up, the decline of $[Ca^{2+}]_i$ during the 'plateau phase' induced by dihydropyridines displayed a biexponential pattern with a 'fast phase' followed by a 'slow phase'. These two phases seem to be dependent on dihydropyridine exposure since their magnitude was related to the increasing concentrations of dihydropyridines. Furthermore, the effect of chirality and ester substitution at position 3 of dihydropyridine enantiomers showed that these structural characteristics may affect the pattern of $[Ca^{2+}]_i$ decay during both the 'fast phase' and the 'slow phase'. In particular, the S-configuration of both nitrendipine and manidipine enantiomers produced a greater $[Ca^{2+}]_i$ decrease during the 'fast phase' than did their R-configuration counterparts. Consequently, the magnitude of this decay during the 'slow phase' was smaller for S-enantiomers than for R-enantiomers. In addition, during the 'slow phase', S-enantiomers induced a faster dose-dependent decay than did R-enantiomers. Patch-clamp experiments also showed the biphasic kinetics of VSCC inhibition by dihydropyridines. This electrophysiological technique also confirmed that the S-enantiomer of both dihydropyridines displayed a faster onset of action and a more pronounced degree of blockade than the respective R-counterpart. The results obtained with both techniques suggested that the S-enantiomers of chiral dihydropyridines such as nitrendipine and manidipine, which bear unsymmetrical substitutions at positions 3 and 5, interact more easily with the receptor site than R-enantiomers (Goldmann and Stoltefuss, 1991), and further supported the idea that the two phases of dihydropyridine-induced $[Ca^{2+}]_i$ decay are likely to correspond to kinetically distinct phases of dihydropyridine-induced VSCC blockade. Whether these two phases of VSCC blockade induced by dihydropyridines correspond to drug binding to separate sites and their physiological relevance to hormone release are currently unknown.

With regard to the role played by the length and lipophilicity of the side chain at position 3 of the dihydropyridine ring, it has been demonstrated that dihydropyridines with stronger and more persistent VSCC blocking activity can be obtained by increasing the volume of the side chain ester substituent (Bossert et al., 1979; Kojda et al., 1991), because this allows for a better interaction with the lipophilic site of the dihydropyridine receptor. The data obtained in the present paper suggest that this substitution can also influence the pattern of VSCC blockade. In fact, both manidipine enantiomers, which possess a longer and more lipophilic 3 side chain substituent, induced a slower $[Ca^{2+}]_i$ decrease than that observed with the respective chiral forms of nitrendipine. Interestingly, and in line with the present observation, Okabe et al. (1987) found that the inhibition of Ca^{2+} currents in smooth muscle cells of rabbit pulmonary artery by manidipine racemate took longer than 10 min to reach a maximum. Similarly, it has been reported that i.v. administration of manidipine racemate, when compared to nitrendipine racemate, induces an antihypertensive effect characterized by a slower onset of action in spontaneously hypertensive rats (Morimoto et al., 1990). Finally, manidipine may have a more prolonged interaction with VSCC than nitrendipine, as suggested by the present electrophysiological findings showing that, upon drug removal, the extent of VSCC blockade remaining after the previous exposure to the S-enantiomer of manidipine was greater than that occurring with the S-enantiomer of nitrendipine.

Collectively, the results of the present study, obtained with the help of single cell microfluorimetry and patch-clamp recordings, demonstrate that the chirality of the carbon at position 4, and the length and lipophilicity of the side chain at position 3 of the dihydropyridine ring can affect the kinetics of VSCC blockade.

Acknowledgements

Special thanks to Dr. Sandra Zavaleta and Mrs. Marcella Donato for their editorial help in the preparation of the manuscript. This work was supported by a grant from the Istituto Superiore di Sanità, Roma, Italy (Progetto sulle proprietà chimico-fisiche dei medicamenti e loro sicurezza d' uso) to P. de Caprariis, by the MURST 60% and the CNR 96.02074, 97.04559 grants to L. Annunziato, and by Telethon 1058, National Research Council (CNR) 97.04512.CT04, 98.03149.CT04 and 97.01233.PF49 to Maurizio Taglialatela.

References

Bossert, F., Horstmann, H., Meyer, H., Vater, W., 1979. Einfluβ der ester-funktion auf die vasodilatierenden eigenschaften von 1,4-dihy-

dro-2,6-dimethyl-4-nitrophenyl-pyridin-3,5-dicarbonsäureestern. Arzneim. Forsch. Drug Res. 29, 226–229.

Cataldi, M., Taglialatela, M., Guerriero, S., Amoroso, S., Lombardi, G., Di Renzo, G.F., Annunziato, L., 1996. Protein tyrosine kinases activate while protein tyrosine phosphatases inhibit L-type calcium channel activity in pituitary GH_3 cells. J. Biol. Chem. 271, 9441–9446.

Delee, E., Jullien, I., Le Garrec, L., 1988. Direct high-performance liquid chromatographic resolution of dihydropyridine enantiomers. J. Chromatogr. 450, 191–197.

Eltze, M., Boer, R., Sanders, K.H., Boss, H., Ulrich, W.-R., Flockerzi, D., 1990. Stereoselective inhibition of thromboxane-induced coronary vasoconstriction by 1,4-dihydropyridine calcium channel antagonists. Chirality 2, 233–240.

Giovannelli, L., Pepeu, G., 1989. Effect of age on K^+-induced cytosolic changes in rat cortical synaptosomes. J. Neurochem. 53, 392–398.

Goa, K.L., Sorkin, E.M., 1987. Nitrendipine: a review of its pharmacodynamic and pharmacokinetic properties, and its efficacy in the treatment of hypertension. Drugs 33, 123–155.

Goldmann, S., Stoltefuss, J., 1991. 1,4-Dihydropyridines: effect of chirality and conformation on the calcium antagonist and calcium agonist activities. Angew. Chem. Int. Ed. Engl. 30, 1559–1578.

Hamill, O.P., Marty, E., Neher, E., Sakmann, B., Sigworth, F.J., 1981. Improved patch-clamp techniques for high-resolution current recording from cells and cell-free membranae patches. Pflüg. Arch. 391, 85–100.

Hockermann, G.H., Peterson, B.Z., Johnson, B.D., Catteral, W.A., 1997. Molecular determinants of drug binding and action on L-type calcium channels. Annu. Rev. Pharmacol. Toxicol. 37, 61–96.

Kajino, M., Wada, Y., Nagai, Y., Nagaoka, A., Meguro, K., 1989. Synthesis and biological activities of optical isomers of 2-(-4-diphenylmethyl-1-piperazinyl)ethyl-methyl 1,4-dihydro-2,6-dimethyl-4-(-3-nitrophenyl)-3-5-pyridinedicarboxylate (Manidipine) dihydrochloride. Chem. Pharm. Bull. 37, 2225–2228.

Keller, E., Nussinovitch, I., 1996. Activity-dependent ultra-slow inactivation of calcium currents in rat anterior pituitary cells. J. Neurophysiol. 76, 2157–2168.

Kojda, G., Klaus, W., Werner, G., Frike, U., 1991. The influence of 3-ester side chain variation on the cardiovascular profile of nitrendipine in porcine isolated trabeculae and coronary arteries. Naunyn-Schmiedegerg's Arch. Pharmacol. 344, 488–494.

Lee, K.S., Tsien, R.W., 1983. Mechanism of calcium channel blockade by verapamil, D600, diltiazem and nitrendipine in single dialysed heart cells. Nature 302, 790–794.

Meguro, K., Aizawa, M., Sohda, T., Kawamatsu, Y., Nagaoka, A., 1985. New 1,4-dihydropyridine derivatives with potent and long-lasting hypotensive effects. Chem. Pharm. Bull. 33, 3789–3797.

Mikus, G., Mast, V., Ratge, D., Wisser, H., Eichelbaum, M., 1995. Stereoselectivity in cardiovascular and biochemical action of calcium antagonist: studies with the enantiomers of the dihydropyridine nitrendipine. Clin. Pharmacol. Ther. 57, 52–61.

Morimoto, S., Hisaki, K., Matsamura, Y., 1990. Effects of manidipine hydrochloride, nisoldipine and nitrendipine on renal hemodynamics and function in stroke-prone spontaneously hypertensive rats (SHRSP). Jpn. Pharmacol. Ther. 18, 2889–2898.

Okabe, K., Terada, K., Kitamura, K., Kuriyama, H., 1987. Selective and long-lasting inhibitory actions of the dihydropyridine derivative, CV-4093, on calcium currents in smooth muscle cells of the rabbit pulmonary artery. J. Pharmacol. Exp. Ther. 243, 703–710.

Okamoto, Y.R., Aburatani, K., Hatada, M., Honda, N., Inotsume, Nakano, M., 1990. Optical resolution of dihidropyridine enantiomers by high performance liquid chromatography using phenylcarbamates of polysaccharides as chiral stationary phase. J. Chromatogr. 513, 375–378.

Ozawa, S., Kimura, N., 1982. Calcium channel and prolactin release in rat clonal pituitary cells: effect of verapamil. Am. J. Physiol. 243, E68–E73.

Scherubl, H., Hescheler, J., 1991. Steady-state currents through voltage-dependent dihydropyridine-sensitive Ca^{2+} channels in GH_3 pituitary cells. Proc. R. Soc. London B Biol. Sci. 245, 127–131.

Stalcup, A.M., Chang, S.C., Armstrong, D.W., Pitha, J., 1990. (*S*)-2-Hydroxypropyl-*b*-cyclodextrin a new chiral stationary phase for reversed-phase liquid chromatography. J. Chromatogr. 513, 181–194.

Tokuma, Y.T., Fujiwara, Noguchi, H., 1987. Determination of (+)- and (−)-nilvadipine in human plasma using chiral stationary-phase liquid chromatography and gas chromatography-mass spectrometry and a preliminary pharmacokinetic study in humans. J. Pharm. Sci. 76, 310–313.

Triggle, D.J., Janis, R.A., 1987. Calcium channels ligands. Annu. Rev. Pharmacol. Toxicol. 27, 347–369.

Van Zwieten, P.A., Pfaffendorf, M., 1993. Similarities and differences between calcium antagonists: pharmacological aspects. J. Hypertens. 11, S3–S11.